Journal of Applied Electrochemistry **33**: 93–100, 2003.

Hydrogen coevolution and permeation in nickel electroplating

L. MIRKOVA[1,*], G. MAURIN[2], M. MONEV[1] and Chr. TSVETKOVA[1]
[1]*Institute of Physical Chemistry, Bulgarian Academy of Sciences, Department 'Elchim', Acad. G. Bonchev, Bl 11, 1113 Sofia, Bulgaria*
[2]*UPR 15 du CNRS 'Physique des Liquides et Electrochimie', Tour 22 , 4 place Jussieu, 75252 Paris Cedex 05, France (*author for correspondence, e-mail address: mirkova@ipchp.ipc.bas.bg)*

Received 24 April 2002; accepted in revised form 14 October 2002

Key words: additives, Devanathan cell, hydrogen permeation, nickel electrodeposition, texture

Abstract

Nickel coatings were electrodeposited onto a steel membrane in a conventional Devanathan cell in order to measure the diffusion rate of hydrogen into the steel substrate during electrodeposition. In most cases a Watts' solution containing various organic additives was used**:** butyne-2 diol-1, 4; saccharine or thiourea. The structure of the electrodeposits was studied by X-ray and Transmission electron microscopy (TEM). It was shown that the electrodeposition parameters (pH, composition of the bath, additives) have a strong effect on hydrogen permeation. The use of organic additives during Ni plating increased the penetration of hydrogen into the substrate. In particular, sulfur-containing additives cause a fast initial increase of the permeation rate, which is attributable to a high surface concentration of H_{ads} when steel is not totally covered with nickel.

By performing permeation experiments with Ni coatings during hydrogen charging from a H_2SO_4 solution, it was shown that hydrogen permeation through nickel coatings is influenced by their fibre texture and by their grain sizes. A low permeation rate was observed in coatings plated in the presence of butyne-2 diol-1,4, which exhibit a strong 100 texture with large grains and a low density of defects. Conversely, the hydrogen diffusion rate is very high in coatings plated in the presence of thiourea or saccharine. These coatings exhibit a weak texture with very small grains.

1. Introduction

Electroplating of nickel coatings, generally used for corrosion protection of steel, proceeds simultaneously with the reaction of hydrogen ion discharge. As a result, atomic hydrogen is formed and adsorbed on the cathodic surface. A major part of the adsorbed hydrogen atoms (H_{ads}) recombines and evolves as molecular hydrogen, and a minor fraction diffuses into the Ni coating and steel substrate. The amount of evolved hydrogen, as well as the amount of permeating hydrogen, can be influenced by many factors such as the nature of the metal, the deposition potential (or the current density), the composition of the solution, the eventual presence of organic additives, and also the pH and the temperature etc. [1–9]. According to [1], it was assumed that metals with a high hydrogen evolution overpotential would have a low degree of hydrogen adsorption, and so, a low amount of codeposited hydrogen. In spite of its low hydrogen overvoltage, nickel has a low amount of codeposited hydrogen due to the high catalytic activity of the metal surface, leading to enhanced recombination and to easy hydrogen evolution.

Several hypotheses were proposed concerning the state of hydrogen in nickel coatings. It may be present as a solid solution of atomic hydrogen [1, 10–12], as atoms absorbed in the subsurface, in active sites, lattice defects or grain boundaries [6]; as hydrates of Ni oxides or salts, as well as in the composition of absorbed organic compounds [13]. Hydrogen atoms, which have directly permeated the steel substrate, or which were occluded into the coating before diffusing into the substrate, can exert detrimental effects on the mechanical properties of steel [14]. Thus, it is important to get a better understanding of this complex phenomenon.

Additives can be of critical importance for the hydrogen permeation process. Their effect on hydrogen coevolution during Ni deposition has been widely studied, but due to the different techniques used, no definite relationships have been found. It is well known [7] that the current efficiency of Ni deposition from a Watts' solution is decreased in the presence of many organic additives such as butyne-2 diol-1, 4 (BD), saccharine (SC) or thiourea (TU) [8]. Knödler observed that hydrogen permeation is greater through bright Ni coatings obtained in a bath containing (BD + SC) than through matte nickel coatings [9]. Additives may affect the gas evolution process by reacting with hydrogen, either by inhibiting the recombination stage (hydrogen

permeation promoters) [15], or by decreasing the rate of proton discharge, thus inducing a decrease in the concentration of absorbed hydrogen in the metal (hydrogen permeation inhibitors) [16]. Other possibilities may be a change in local pH, or an increase in the partial hydrogen current, finally leading to enhanced formation of Ni hydroxides in the cathodic layer [2].

Most additives exert a strong effect on the structure of Ni deposits causing grain refinement and changing the preferred orientation of growth as well as the grain morphology. It has been shown by Amblard et al. [17–19] that the preferred orientation of Ni deposits depends on the cathodic layer composition, that is, on interfacial species such as H_2, H_{ads} or $Ni(OH)_2$ which are formed during the cathodic process as a consequence of hydrogen coevolution. The predominance of a given species depends on plating conditions, mainly pH, current density, temperature and bath composition. The activity of organic additives has been ascribed to the role they play in the Ni^{2+}/H^+ competition [18]. Moreover, the additives may act in a different way depending on the preferred orientation, since their adsorption depends on the crystallographic planes, which constitute the facets of the deposit [17]. On the other hand, the internal structure of the deposits may strongly affect the hydrogen permeation. Paatsch [20] has suggested that the hydrogen permeation rate could be related to the various textures of Ni coatings obtained at different current densities in a Watts' electrolyte. However, until now, no clear relationship between hydrogen permeation and the structure of Ni coatings obtained in the presence of additives, has been established.

The aim of this work is to study the effect of nickel coatings on hydrogen permeation into a steel foil. For this purpose, Ni coatings were electrodeposited from electrolytes containing various organic inhibitors, which are known to modify the nickel texture. Hydrogen coevolution and permeation were studied during Ni electrodeposition, and afterwards, during electrochemical hydrogen charging in sulfuric acid solution within a conventional Devanathan cell. The texture and the internal structure of the Ni coatings were characterized by various techniques.

2. Experimental conditions

Most nickel coatings were obtained at room temperature from a Watts' electrolyte (0.89 M $NiSO_4 \cdot 7H_2O$, 0.21 M $NiCl_2 \cdot 6H_2O$ and 0.49 M H_3BO_3; pH between 1.2 and 3.6). Some experiments were performed in all-sulfate or all-chloride nickel electrolytes at pH 3.6. The amount of Ni^{2+} ions (64.65 g dm^{-3}) was the same in all electrolytes. All reagents were of analytical grade. The following organic compounds were added to the Watts' electrolyte separately or in a combination: butyne-2 diol-1, 4: 0.2 g l^{-1} (2.3 mM); saccharine: 1.0 g l^{-1} (5.5 mM); and thiourea: 0.2 g l^{-1} (2.6 mM). Also,

$$\text{Butyne} - 2\ \text{diol} - 1,4(0.2\,\text{gl}^{-1}) + \text{Saccharine}(1.0\,\text{gl}^{-1})$$

The effective amount of molecular hydrogen, evolved during Ni deposition, was measured by using a special bell-type cell, described elsewhere [21]. The rate of hydrogen permeation into the steel substrate during Ni electrodeposition was evaluated by the method of Devanathan and Stachurski [22], as in previous work related to hydrogen permeation during Zinc electrodeposition onto steel [23]. The set-up was made of two symmetrical electrochemical cells mounted on both sides of the horizontal steel membrane. Both cells were equipped with a platinum grid as counter electrode. The upper (entry) side of the membrane was subjected to cathodic nickel electroplating. Conversely, the lower (exit) side, pre-coated with a thin Pd layer, was polarized anodically in order to oxidize the hydrogen which diffused through the substrate. The ionization current, recorded under potentiostatic control against a Hg/HgO reference electrode, was a direct measure of the permeation rate I_p.

Steel membranes were prepared from a 100 μm thick cold-rolled sheet of low carbon mild steel (Willy Traub, GmbH). It has been shown previously [24] that the permeation rate depends strongly on the preliminary heat treatment of the steel membrane, in relation to the density of crystal defects. The diffusion coefficient was higher by one order of magnitude after annealing. In the present experiments, the membrane was carefully annealed at 500 °C in vacuum for 2 h. Before each experiment, the membrane was degreased in acetone, rinsed, ultrasonically cleaned in ethanol and etched in 5 M HCl. Then, the exit side was electroplated with a continuous palladium layer (thickness 1.2 μm). Finally, the membrane was cathodically degreased for 30 s, rinsed and mounted between the cells. The exposed area was 2 cm^2 on both sides. A 0.5 M NaOH solution was introduced into the ionization cell and a −150 mV vs Hg/HgO potential was applied to reduce the surface oxides. Then, the potential was shifted to +150 mV for a time sufficiently long to get a residual anodic current density lower than 1 $\mu A\ cm^{-2}$. After this preliminary treatment, the electrolyte was introduced into the polarization cell and nickel electrodeposition was started on the upper side at a constant cathodic current density (c.d.) of 20 mA cm^{-2}. The permeation current was recorded against time until a steady state. In separate experiments, the membranes, pre-coated with a 12 μm Ni layer, were submitted to hydrogenation in a 0.5 M H_2SO_4 solution under a galvanostatic regime at 10 mA cm^{-2}.

The texture of 50 μm thick Ni layers were studied by X-ray diffractometry. The axis of the preferred orientation was identified by comparing the diffraction peak intensities with that of the ASTM data given for a randomly oriented sample. For the purpose of transmission electron microscopy observations of the nickel

coatings, thin foils were prepared by electrochemical dissolution in a 'Struers Tenupol' apparatus.

3. Results and discussion

3.1. *Influence of pH and bath composition on hydrogen permeation*

Figure 1(a) shows hydrogen permeation transients obtained during Ni plating in Watts' electrolyte at pH 1.2; 2; 3; 3.6 and 4. During the initial stage, I_p abruptly increases before reaching a steady value I_pst, which stays practically constant for over one hour, although a continuous decrease might be expected due to the increase in coating thickness. We previously observed a similar phenomenon during zinc electrodeposition [23]. It may be assumed that the penetration of H into steel at the steel/coating interface contributes to the limitation of the overall permeation rate through the combined membrane.

At pH 1.2, the nickel current efficiency was very low and the first transient had a similar form to transients obtained previously when charging a steel membrane in a KCl solution [24]. In particular, the presence of a maximum on the transient was ascribed to a saturation effect of hydrogen in the bulk material. For pH 2, the steel was well covered with nickel, and it can be observed that the mean slope of the rising part, as well as the steady state permeation rate I_pst, were decreased. In Figure 1(b), the values of I_pst are plotted as a function of pH. I_pst decreased rapidly in the pH range 1.2–2, before becoming nearly constant for pH > 3. It can be assumed that the permeation current through the steel/nickel combined membrane is strongly related to the partial hydrogen current on the entry side, which is very sensitive to pH. This assumption is in agreement with literature data on effects of pH on hydrogen incorporated into Ni layers [5], and also on the current efficiency [4].

The permeation transients obtained during Ni plating in Watts' electrolyte were compared with those corresponding to all-sulfate or all-chloride nickel electrolytes at pH 3.6. Figure 2 shows that the permeation rate is much smaller when Watts' bath is used. In the case of all-chloride bath, the sharp rise of I_p at the beginning and the steady state value I_pst may be ascribed to the higher hydrogen evolution rate due to the lower hydrogen over-potential. It has also been suggested that the reaction $H_{ads} \rightarrow H_{abs}$ is enhanced in the presence of specifically adsorbed Cl^- ions [25]. At this high permeation rate, the occurrence of a maximum on the transient curve indicates a saturation effect within the metal. The experimental values of I_pst decreased in the following order: all-chloride; all-sulfate and Watts' electrolyte. The quantity Q_H of hydrogen, permeating the steel membrane during 12 min plating, was calculated by integrating the permeation transients I_p/t. The value of Q_H for all-chloride electrolyte (57.2×10^{-9} M cm^{-2}) was about 1.5 times larger than that corresponding to the all-sulfate electrolyte (37.9×10^{-9} M cm^{-2}), and about three times larger than that corresponding to the Watts' electrolyte (19.8×10^{-9} M cm^{-2}). Raub and Sauter, observed a similar effect of the bath composition on the quantity of hydrogen included in nickel coatings, in the 1 to 5 pH range. This quantity was much larger in deposits obtained from an all-chloride electrolyte than from all-sulfate electrolyte [5].

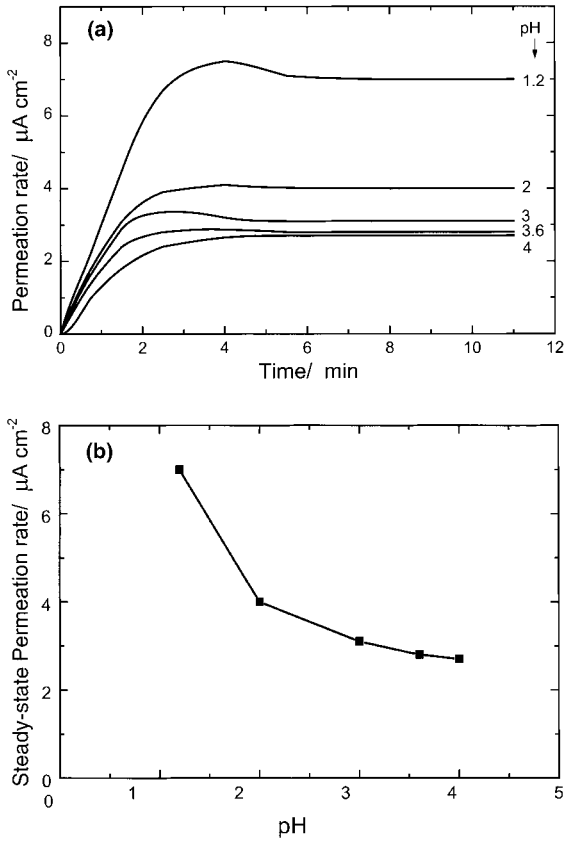

Fig. 1. (a) Hydrogen permeation transients obtained during Ni plating on steel in Watts' electrolyte at pH 1.2, 2.0, 3.0, 3.6 and 4.0. (c.d. 20 mA cm^{-2}). (b) Steady-state hydrogen permeation rate against pH values.

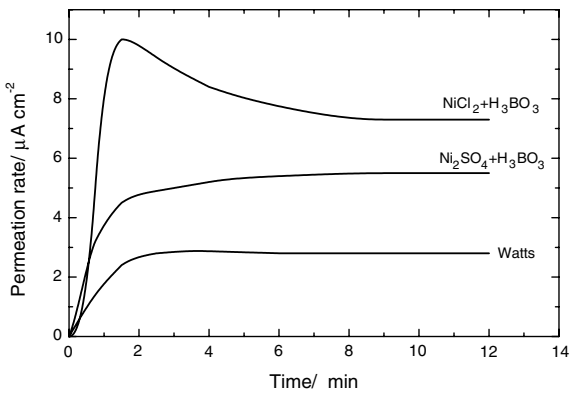

Fig. 2. Hydrogen permeation transients obtained during Ni plating on steel in Watts', all-sulfate and all-chloride electrolyte at pH 3.6 (c.d. 20 mA cm^{-2}).

3.2. *Influence of organic additives on hydrogen coevolution and permeation*

The current efficiency of Ni deposition η_{Ni} from the Watts' electrolyte containing the different additives was measured gravimetrically in a cell with a vertical steel cathode in identical experimental conditions as in the Devanathan cell (room temperature, no agitation). The partial hydrogen contribution $\eta_H = 1 - \eta_{Ni}$ was deduced and is reported in Table 1. For both pHs, the values of η_H were systematically the lowest for the additive-free electrolyte. At pH 3.6, the highest value of η_H was observed in the presence of (SC + BD). At pH 1.2, the coatings were irregular, with cracks and scales. The values of η_H were much higher than at pH 3.6 and the relative effects of additives were more pronounced. In this case, much of the total current was consumed in hydrogen formation, especially in the presence of TU; SC or (SC + BD). These results are in agreement with literature data for decreased current efficiency of Ni deposition in the presence of BD [7, 26] and in the presence of SC or TU [8].

The time dependence of the volume of hydrogen (V_H in ml at atmospheric pressure), formed during Ni deposition (pH 1.2; 20 mA cm^{-2}) and evolved as bubbles is shown in Figure 3. The values of V_H were always larger in the presence of additives, in particular in the presence of S-containing additives (SC + BD, SC, TU). By taking into account that a part of the evolved hydrogen is dissolved in the electrolyte, the results agree reasonably with the above data for η_H obtained at pH 1.2. However, at pH 3.6, the volume of evolved hydrogen was too small to obtain measurements with a sufficient accuracy.

Figure 4(a) and (b) show the permeation curves obtained during Ni plating in Watts' electrolyte with and without additives at pH 3.6 and pH 1.2, respectively. A similarity in the positions of the corresponding curves is observed on both Figures. It is noteworthy that the largest permeation rates were obtained in the presence of thiourea, although according to measurements of η_H or V_H (Figure 3), the partial current of hydrogen evolution was not the largest. The values of the permeation rate were systemically lower at pH 3.6 and for the pure Watts' solution. In all cases, the permeation rate rose rapidly at the beginning of Ni deposition and gradually reached a steady value, although the coating thickness was continuously increasing. In the presence of TU at pH 3.6, I_p passed through a sharp initial peak before returning to the usual curve. It has been suggested in [27], that in a short initial stage, the permeation rate is predominantly controlled by the coverage of the steel surface with H_{ads} and by the permeability of the steel itself. During the following

Table 1. Partial hydrogen contribution η_H (in %) for the Watts' electrolyte without and with additives (c.d. 20 mA cm^{-2}; 25 °C; no agitation)

Watts' electrolyte	Without additive	+BD	+SC	+(SC + BD)	+TU
pH 3.6	0.6	1.2	2.6	3.9	2.9
pH 1.2	37.4	46.7	84.6	84.9	93.0

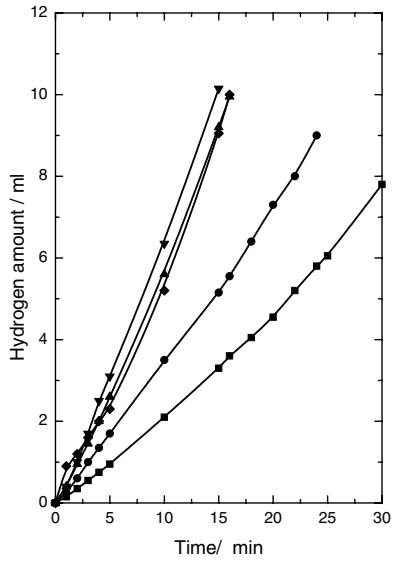

Fig. 3. Hydrogen amount evolved in the atmosphere during Ni plating on steel in Watts' electrolyte without additive or with (●) BD or (▲) SC or (▼) (SC + BD) or (♦) TU at pH 1.2 (c.d. 20 mA cm^{-2}). Legend: (■) Watts.

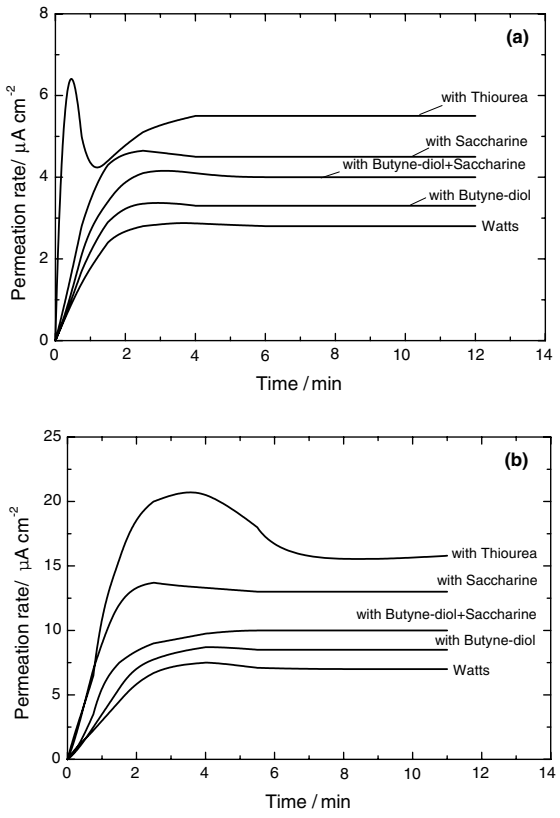

Fig. 4. Hydrogen permeation transients obtained during nickel plating on steel in Watts' electrolyte without additive or with BD or SC or (SC + BD) or TU (c.d. 20 mA cm^{-2}). (a) pH 3.6 and (b) pH 1.2.

stage, hydrogen permeation into the steel substrate becomes controlled by the hydrogen coverage, by the permeability and by the barrier efficiency of the nickel coating. Thus, according to this hypothesis, the sharp initial rise observed in the presence of S-containing additives, especially in the case of TU, would be due to a high surface concentration of H_{ads} on the steel surface or to a higher penetration rate, induced by the presence of these inhibitors.

As soon as an appreciable amount of nickel is deposited, a barrier against the diffusion of hydrogen is formed [27, 28]. The steady-state permeation rate gives an indication of the attainment of a constant hydrogen coverage, and also gives an idea of the permeability of the coating. The values of I_pst, as well as the total amount of hydrogen Q_H crossing the membrane during 12 min of plating in various baths, are given in Table 2. The steady hydrogen flow I_pst as well as Q_H increased in the following order: without additive, +BD, +(BD + SC), +SC, +TU.

The higher values of I_pst, and Q_H obtained in the presence of the various inhibitors may result from the larger partial hydrogen current density, from the smaller thickness of the coating and also from the higher diffusion rate due to structural modifications of the coatings. Both quantities were larger in the presence of Sulfur-containing additives than in the presence of BD or in the absence of additives. S-containing additives have been previously recognized as promoters of hydrogen permeation during electroplating [9]. According to [29], they are usually chemi-sorbed on the metal surface and by inhibiting the recombination reaction of hydrogen atoms into molecular hydrogen, they increase the surface coverage of adsorbed atomic hydrogen, which is considered as the driving force for hydrogen permeation.

3.3. *Correlation between the permeability of Ni coatings and their structure*

To verify the validity of above hypothesis, nickel coatings of a constant thickness were deposited on the steel membrane from the Watts' electrolyte containing tested additives (pH 3.6). The structure of Ni coatings was studied by X-ray diffractometry and by transmission electron microscopy (TEM) (Figures 5 and 6).

Table 2. Steady-state permeation rate I_pst and total quantity of hydrogen Q_H permeating the steel membrane during 12 mn of Ni deposition in Watts' electrolyte without and with various additives; (c.d. 20 mA cm^{-2}; pH 3.6 or 1.2)

	I_pst/μA cm^{-2}		$Q_H/10^{-9}$ mol cm^{-2}	
	pH 3.6	pH 1.2	pH 3.6	pH 1.2
Without additive	2.8	7.0	19.8	48.3
With butyne-diol	3.3	8.5	23.3	57.7
With saccharine	4.5	13.0	32.3	92.9
With butyne-diol + saccharine	4.0	10.0	28.4	68.0
With thiourea	5.5	15.9	40.6	121.3

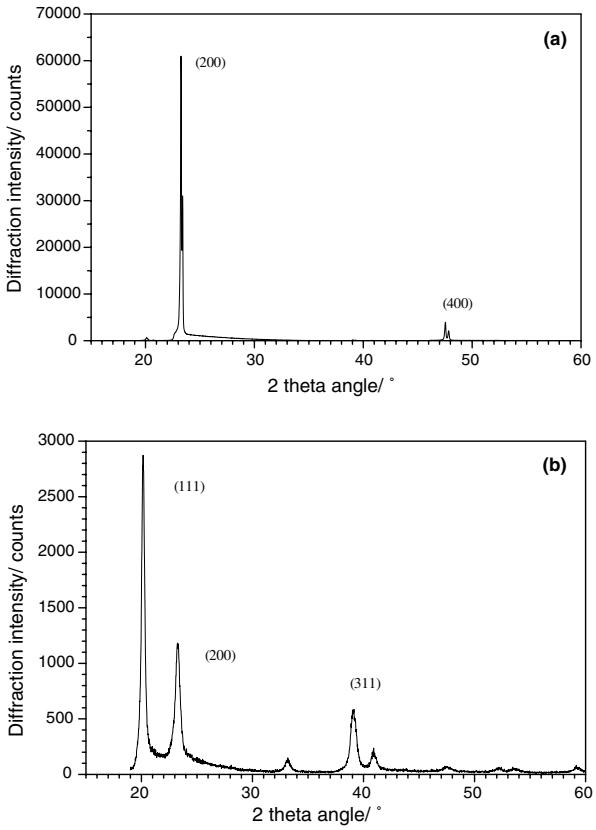

Fig. 5. X-ray diffraction patterns of nickel electrodeposits obtained in Watts' electrolyte (pH 3.6; c.d. 20 mA cm^{-2}) in the presence of (a) butyne-diol and (b) saccharine.

In the absence of additive, the coatings are dull, with a weak ⟨2 1 0⟩ preferred orientation. That is in agreement with previous results [18, 30], according to which the ⟨2 1 0⟩ texture axis is characteristic of a strong inhibition by molecular H_2, especially at low pH. It was demonstrated that the growth of this texture involves a complex helical organization of (1 1 1) twin planes [31]. It can be assumed that the twin plane network realizes a continuous path from the bottom to the top of the columnar grains, which constitute the nickel coating. Surprisingly, when BD was added, a very strong ⟨1 0 0⟩ texture was observed (Figure 5(a)), whereas this texture was known to be characteristic of a low inhibition state when a stirred Watts' solution at moderate temperature was used [17, 18, 30]. In the present experimental conditions (room temperature, absence of agitation), the partial hydrogen current was small and it could be assumed that hydrogenation of adsorbed BD molecules contributes to reduced hydrogen coverage, thus promoting the ⟨1 0 0⟩ texture. In the presence of SC or (BD + SC), the coatings were mirror-bright and the structure was changed into a mixture of weak ⟨3 1 1⟩ and ⟨1 1 1⟩ textures (Figure 5(b)). These textures are characteristic of very strong inhibition [18]. In the presence of TU, the coatings were also mirror-bright, and weak ⟨1 0 0⟩ and very weak ⟨3 1 1⟩ textures were detected.

TEM micrographs of coatings deposited in the presence of BD (Figure 6(a)), show large grains (mean

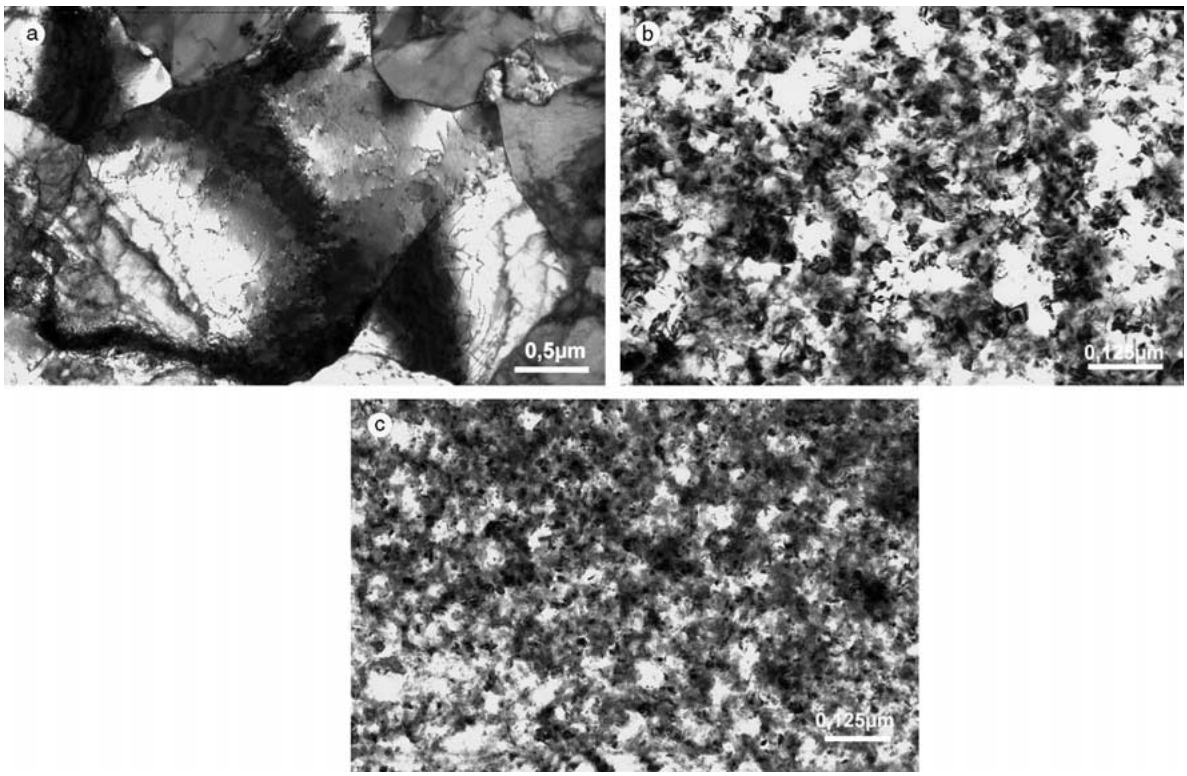

Fig. 6. TEM micrographs of nickel electrodeposits obtained in a Watts' electrolyte in the presence of various additives (pH 3.6; c.d. 20 mA cm^{-2}). (a) butyne-diol, (b) saccharine and (c) thiourea.

dia. ~2 μm) with a low density of dislocations or twin lamellae with the characteristic aspect investigated for the $\langle 1\,0\,0 \rangle$ texture [30]. The twin planes are randomly distributed and there is no continuous path throughout the columnar grains. For coatings deposited in the presence of SC or (BD + SC), the grain size was considerably decreased (mean dia. ~0.03 μm) (Figure 6(b)). Crystal details are still visible on the micrographs. A large defect density was observed. In the presence of TU, the grain size was in the same order of magnitude, but the crystal details were difficult to observe (Figure 6(c)), because of additional contrasts due to strong internal stresses, caused by inclusion of impurities, most probably sulfur-containing impurities.

Additional permeation experiments were carried out with steel membranes coated with the various types of nickel electrodeposits, but the upper cell of the Devanathan set-up was filled with a 0.5 M H_2SO_4 solution. Hydrogen was evolved at a constant current density of 10 mA cm^{-2}. Permeation transients are presented in Figure 7 and the total amounts of hydrogen Q_H crossing the membrane during hydrogenation of the coatings are given in Table 3. The texture and the surface aspect of the deposits are also reported. As seen in Figure 7, during these hydrogenation experiments, coatings deposited in the presence of the various additives showed lower I_pst as compared with additive-free electrolyte. This effect was particularly important with coatings deposited in the presence of BD. In addition, a delay was present at the beginning of polarization. In contrast, for deposits prepared in the presence of sulfur-containing additives, I_p was strongly accelerated at the beginning of polarization. This effect was particularly vigorous in the presence of TU, where I_p passed through a sharp maximum before reaching a steady value, thus contributing to the high value of Q_H (Table 3). It is noteworthy that Q_H was not clearly related to the surface aspect of the nickel coatings as proposed by Knödler [9].

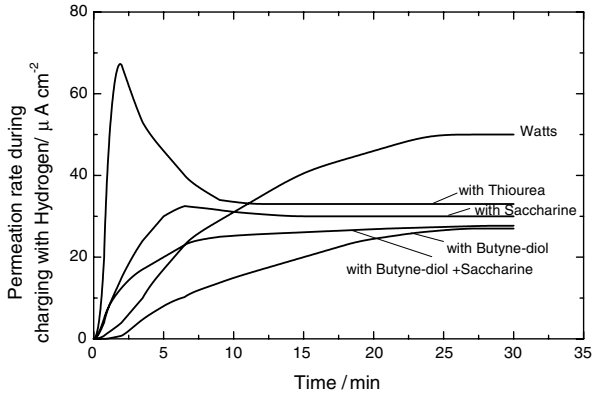

Fig. 7. Permeation transients obtained during charging of Ni coatings on steel with hydrogen at c.d. 10 mA cm^{-2} in 0.5 M H_2SO_4. (Ni coatings were obtained in Watts' electrolyte without additive or with BD or SC or (SC + BD) or TU at pH 3.6; c.d. 20 mA cm^{-2}).

Comparison between hydrogen permeation data and X-ray or TEM observations suggests that the crystal structure of the nickel coatings has a strong effect on the permeation process. In the presence of BD, the high quality of the texture and the low defect density, are associated with a low hydrogen steady state permeation

Table 3. Texture and surface aspects of coatings obtained in Watts' electrolyte without and with additives (c.d. 20 mA cm^{-2}; 25 °C; pH 3.6). Total hydrogen quantity Q_H permeating 12 μm Ni layers on steel during 30 min of hydrogenation in 0.5 M H_2SO_4 (c.d 10 mA cm^{-2})

	Texture	Surface aspects	$Q_H/10^{-7}$ mol cm^{-2}
Without additive	⟨2 1 0⟩ + ⟨1 1 0⟩ weak	dull	6.6
With butyne-diol	⟨1 0 0⟩ very strong	dull	3.4
With saccharine	⟨3 1 1⟩ + ⟨1 1 1⟩ very weak	mirror-bright	5.3
With butyne-diol + saccharine	⟨3 1 1⟩ + ⟨1 1 1⟩ very weak	mirror-bright	4.5
With thiourea	⟨1 0 0⟩ very weak	mirror-bright, non-adherent	6.9

rate, which can be attributed to a lower diffusion coefficient in the nickel coating. Conversely, in the case of coatings deposited in the presence of the other additives, the rich density of grain boundaries and crystal defects, resulting from the small grain size, is correlated with a higher permeation rate.

The effect is more complex in the presence of TU, where, in agreement with Latanision and Opperhauser [32], it can be assumed that sulfur inclusions promote hydrogen entry, thus contributing to the fast initial rise of I_p (Figure 7). Smialowski has attributed this phenomenon to a decrease in the energy bond between the surface metal atoms by S^{2-} chemisorption [33]. Conway et al. [34] suggested that adsorbed organic species may modify the kinetic equilibrium between H_{ads} coverage and the hydrogen concentration in the sublayer, thus promoting hydrogen permeation into the matrix. It has been reported that nickel foils, obtained in the presence of napthalene–trisulfonic acid, in the initial stage of charging with hydrogen, exhibited a permeability so high that this material could be used as a substitute for palladium [35]. It can be assumed that napthalene–trisulfonic acid and TU have a similar effect on hydrogen penetration.

The decrease of I_p after the maximum on the permeation curve (Figure 7) results from hydrogen trapping, especially in the sublayer region. It can be assumed that the mechanical stresses revealed by TEM observations, contribute to this trapping effect. It has been observed that segregation of metalloids in the grain boundaries is responsible for absorption of large amounts of hydrogen [36, 37].

It is difficult to verify these assumptions by using steel/nickel combined membranes. Thus, new permeation experiments are presently being performed in the Devanathan cell using nickel electrodeposits, separated from their substrate. The effect of TU addition to the electrolyte on direct hydrogen penetration into steel is also under investigation.

4. Conclusion

The rate of hydrogen permeation into a low carbon steel substrate was measured by the Devanathan–Stachurski method during nickel electroplating. It was observed that the electrodeposition parameters have a strong influence on hydrogen permeation. It can be concluded that the permeation rate increases when the electrodeposition conditions give a low current efficiency, that is to say, a high hydrogen evolution rate at the nickel deposit surface. For example, the steady-state permeation rate through the steel membrane increased sharply when the pH of the Watts' bath was decreased from 4 to 1.2 or when an all-sulfate or all-chloride bath was used instead of a Watts' bath. Addition of organic inhibitors to the plating bath also has a deleterious effect on the nickel current efficiency, and consequently induces a high permeation rate through the steel/nickel system.

However, the plating conditions and additives may also influence structural characteristics of nickel coatings, such as the crystal axis of the texture, the grain size, the presence of crystal defects with peculiar spatial organization and the internal stresses. All these parameters may have an effect on the diffusion and trapping processes of hydrogen in the nickel layer. The influence of nickel structure was demonstrated by performing Devanathan–Stachurski experiments, when nickel coatings supported by a steel membrane, were charged with hydrogen at constant rate. Nickel layers prepared in the presence of BD are less hydrogenated because of their strong ⟨1 0 0⟩ preferred orientation, their large grain size and their low crystal defect density. Conversely, coatings deposited in the presence of S-containing additives, especially TU, exibit high hydrogen permeability in relation to their very weak preferred orientation and the high density of grain boundaries due to the small grains. It can be assumed that sulfur inclusions promote the penetration of hydrogen into the metal sublayer thus enhancing the permeation rate at the beginning of the process, but they also contribute to hydrogen trapping in grain boundaries, thus limiting the steady state diffusion current.

Acknowledgements

This work was supported by the Bulgarian Academy of Sciences (Bulgaria) and the Centre National de la Recherche Scientifique (France) in the framework of a cooperative research program.

References

1. A.T. Vagramian and Z.A. Soloveva, 'Metodi issledovania electroosajdenia metallov' (Izd. Academmii nauk, Moskva, 1960), p. 249 (in Russian).

2. Yu.Yu. Matulis (Ed.), 'Bright Electrolytic Coatings' (Mintis, Vilnius, 1969), p. 612 (in Russian).
3. Th.C. Franklin and J.R. Goodwyn, *J. Electrochem. Soc.* **109** (1962) 288.
4. E. Mantzell, *Z. Electrochem.* **43** (1937) 174.
5. E. Raub and F. Sautter, *Metalloberfläche* **13** (1959) 129.
6. Ch.J. Raub, *Plat. Surf. Finish.* Sept. (1993) 30.
7. E. Raub, A. Knödler, A. Disam and H. Kawase, *Metalloberfläche* **23** (1969) 293.
8. M. Monev, M.E. Baumgärtner and Ch.J. Raub, *Metalloberfläche* **51** (1997) 328.
9. A. Knödler, *Metalloberfläche* **40** (1986) 515.
10. T. Boniszewski and G. Smith, *J. Phys. Chem. Solids* **21** (1961) 115.
11. R.Y .Rokes and R.H. Emmett, *J. Am. Chem. Soc.* **81** (1959) 5032.
12. O.C. Popova and K.M. Gorbunova, *J. Phizicheskoi Himii* **32** (1958) 2020 (in Russian).
13. A.L. Rotinian and E.Sh. Ioffe, *J. Prikladnoi Himii* **33** (1960) 362 (in Russian).
14. C.M. Beloglazov, 'Hydrogenation of Steel During Electrochemical Processes' (Leningrad University Press, Leningrad, 1975), p. 278 (in Russian).
15. Th.C. Franklin, *Plat. Surf. Finish.* Apr. (1994) 62.
16. M.H. Abd Elhamid, B.G. Ateya and H.W. Pickering, *J. Electrochem. Soc.* **144** (1997) L58.
17. I. Epelboin, M. Froment and G. Maurin, *19th Meeting of the International Committee of Electrochemical Thermodynamics and kinetics* (C.I.T.C.E.), Detroit, MI, Sept. (1968), p. 1.
18. J. Amblard, I. Epelboin, M. Froment and G. Maurin, *J. Appl. Electrochem.* **9** (1979) 233.
19. C. Kollia, N. Spyrellis, J. Amblard, M. Froment and G. Maurin, *J. Appl. Electrochem.* **20** (1990) 1025.
20. W. Paatsch, *Plat. Surf. Finish.* Aug. (1988) 52.
21. M. Monev, L. Mirkova, I. Krastev, Hr. Tsvetkova, St. Rashkov and W. Richtering, *J. Appl. Electrochem.* **28** (1998) 1107.
22. M.A.V. Devanathan and Z. Stachurski, *Proc. Roy. Soc. Lond.* **A 270** (1962) 90.
23. L. Mirkova, G. Maurin, I. Krastev and Hr. Tsvetkova, *J. Appl. Electrochem.* **31** (2001) 647.
24. G. Maurin, L. Mirkova and M. Monev, Proceedings of the Third International Congress on 'Mechanical Engineering Technologies'01', Ed. Sci. Technol. Union of Mechanic. Engineering, Sofia, 24–26. June (2001), JanVIII, 2(57), p. 298.
25. H. Liebscher, *Jahrbuch Oberflächentechnik* **52** (1999) 31.
26. E. Raub and K. Muller, *Metalloberfläche* **18** (1964) 161.
27. M.A.V. Devanathan, Z. Stachurski and W. Beck, *J. Electrochem. Soc.* **110** (1963) 886.
28. S. Venkatesan, R. Subramanian and M.A.V. Devanathan, *Metal Finish.* May (1966) 50.
29. E.G. Dafft, K. Bohnenkamp and H.J. Engell, *Corros. Sci.* **19** (1979) 591.
30. J. Amblard, M. Froment and N. Spyrellis, *Surf. Technol.* **5** (1977) 205
31. J. Amblard, G. Maurin, D. Mercier and N. Spyrellis, *Scripta Met.* **16** (1982) 579.
32. R.M. Latanision and H. Opperhauser, *J. Met. Trans.* **5** (1974) 483.
33. M. Smialowski, *Zashtita Metallov* **3**(3) (1967) 267 (in Russian).
34. B.E. Conway and G. Jerkiewicz, *J. Electroanal. Chem.* **357** (1993) 47.
35. D. Engelhaupt, US Patent US 4 290 858 (22 Sept. 1981).
36. R.M. Latanision and M. Kurkela, *Corrosion* **39**(5) (1983) 174.
37. S.M. Bruemmer, R.H. Jones, M.T. Thomas and D.R. Baer, *Scripta Met.* **14** (1980) 1233.